World Academy of Science, Engineering and Technology
International Journal of Geotechnical and Geological Engineering
Vol:18, No:10, 2024

In-Plane Shear Tests of Prefabricated Masonry Panel System with Two-Component Polyurethane Adhesive

E. Fehling, P. Capewell

Abstract**—**In recent years, the importance of masonry glued by polyurethane adhesive has increased. In 2021, the Institute of Structural Engineering of the University of Kassel was commissioned to carry out quasi-static in-plane shear tests on prefabricated brick masonry panel systems with 2K PUR adhesive in order to investigate the load-bearing behavior during earthquakes. In addition to the usual measurement of deformations using displacement transducers, all tests were documented using an optical measuring system, which was used to determine the surface strains and deformations of the test walls. To compare the results with conventional mortar walls, additional reference tests were carried out on test specimens with thin-bed mortar joints. This article summarizes the results of the test program and provides a comparison between the load-bearing behavior of masonry bonded with polyurethane adhesive and thin-bed mortar in order to enable realistic non-linear modeling.

Keywords**—**Glued Masonry, in-plane tests, shear resistance, polyurethane adhesive.

I. Introduction

The use of glued masonry has increased in recent years. Glued masonry is generally assigned lower strength values than the mortared masonry types, whereby only a few test results are available so far, especially for the shear load-bearing capacity in plane, which makes it more difficult to get a realistic assessment of the seismic load-bearing behavior of the glued masonry. Therefore, experiments were carried out at the Department of Concrete Structures at University of Kassel to investigate the shear load-bearing capacity of prefabricated floor-to-ceiling wall panels with two-component polyurethane adhesive using quasi-static cyclic tests. All tests carried out were documented with the optical measuring system ARAMIS (GOM GmbH, Braunschweig, Germany), which records the strains and displacements of the wall surface during the wall tests and thus enables more reliable statements to be made about the failure modes present. The tests are documented in detail in the research report [1].

II. Test Program

As part of the research project, a total of four test panel systems with glued horizontal joints of two-component polyurethane adhesive (PU) and three reference walls manufactured using thin-bed mortar (TBM) were tested. The glued wall elements were prefabricated in a precast plant and then delivered to the University of Kassel. Then they were each placed on a concrete beam with a mortar bed joint. To transfer the load, a stiff steel composite beam was also laid in a bed of mortar on the top of each wall panel. The mortar layers on the top and bottom of the panels were allowed to cure for at least three weeks prior to testing. The reference walls, manufactured using the TBM, were set up directly in the laboratory at the University of Kassel and were also allowed to harden for three weeks before testing. The wall height of all test walls was between 2.52 m and 2.55 m, on average 2.54 m. Fig. 1 shows the type of the vertical perforated brick stone used, which is sold under the trade name "Coriso W07". In Fig. 2 one can see the prefabrication of the glued masonry panels in the precast plant. According to the product data sheet, the nominal thickness is 0.365 m. The stones of all walls tested were part of same batch. The stone compressive strength perpendicular to the horizontal joint was determined in tests according to DIN EN 772-1:2016-05 [2] with an average of 8.5 N/mm^2. The masonry compressive strength of the two masonry types was determined according to DIN EN 1052-1:1998-12 [3] in tests with 3.0 (TBM) and 2.9 (PU). All test walls have the same geometric dimensions. The vertical loading and the degree of moment fixture were varied (in the follow-up test W2.2, the moment zero crossing was shifted upwards). To simulate the partial support of masonry walls at typical wall-floor connections, the slab bearing length was also varied in the test program (head and bottom with the same slab bearing length).

Fig. 1 Tested type of prefabricated bricks

E. F. is with the Department of Concrete Structures, University of Kassel, Kurt-Wolters-Straße 3, 34109 Kassel, Germany (e-mail: fehling@uni-kassel.de).

P.C. is with the Department of Concrete Structures, University of Kassel, Kurt-Wolters-Straße 3, 34109 Kassel, Germany (e-mail: capewell@uni-kassel.de).

Fig. 2 Application of the two-component adhesive in the precast plant [4]

III. Test Performance

The biaxial test setup of the Institute for Structural Engineering at the University of Kassel was used to carry out the tests, see Figs. 3 and 4. The test setup is operated by a total of three hydraulic cylinders: two vertical cylinders from above and one horizontal cylinder from the side. During the tests, the vertical load was kept constant as the sum of the forces applied by the two vertical cylinders. The moment restraint at the head of the wall was simulated with the vertical cylinders by an additionally applied force couple depending on the horizontal force and the intended position of the moment zero crossing. The tests were run displacement controlled. The horizontal wall head displacements were applied sinusoidally with a constant period of at least 120 seconds as a function of the test time. After each three cycles, the displacement amplitude was increased. Fig. 5 gives an overview of the measuring points. For the measurement with the optical measuring system, all test walls (except W3) were provided with a black and white pattern.

Fig. 3 Test setup: test wall

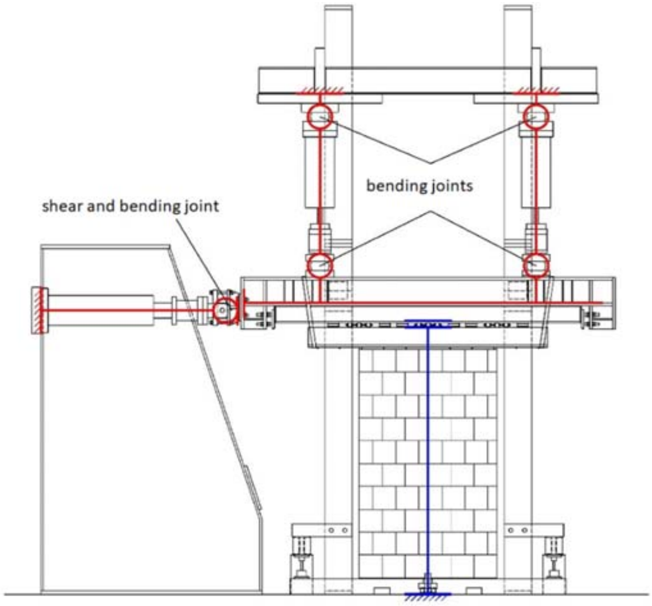

Fig. 4 Test setup: static system

IV. Test Results and Observations

The essential test results are summarized in Table I. In addition, the characteristic shear resistances according to EC6/NA (D) [5] are also included for comparison. For all experimentally determined load-deformation curves, a bilinear approximation was also created using Tomazevic's method [6].

The experiments W1.t and W1.3 as well as W2.1 and W2.2 were each carried out on the same test wall. As a consequence of this, pre-damage can be expected at the beginning of the test in tests W1.3 and W2.2. This must also be taken into account in the optical measurement data from test W2.2.

For all tests from the test data, a primary shear failure can be assumed. According to the hysteresis and the optical measurement data, a secondary flexural failure can be assumed for the TBM walls, which explains the constricted hysteresis (more on this in the interpretation of the results). Furthermore, a distinction must be made between the front and rear of the partially supported walls (W3, W4, W7). Stepped frictional failure was usually evident on the protruding front side. A diagonal tension failure was evident on the reverse side with full support. This can be explained by the non-uniform normal stress distribution over the wall thickness as a result of the partial support and was already observed by Pfetzing in [7].

When comparing the test results W2.2 and W3, or W4 and W6, it is noticeable that a lower slab bearing length leads to a reduction in the load-bearing capacity and the deformation capacity, which also corresponds to observations by Pfetzing in [7]. The hysteresis and the vertical displacement in the middle of the wall head (Figs. 6, 8, 10) and the main strain distributions (Figs. 7, 9, 11) approximately at the time when the respective maximum forces were reached, documented with the optical measuring system, are shown below, for the three test pairs with the same geometry, load, slab bearing depth and bending moment fixture but different bed joint. Test W3 was carried out without a surface pattern, so that a strain measurement of the wall surface was not possible here and the displacement of the wall surface was only documented in discrete points.

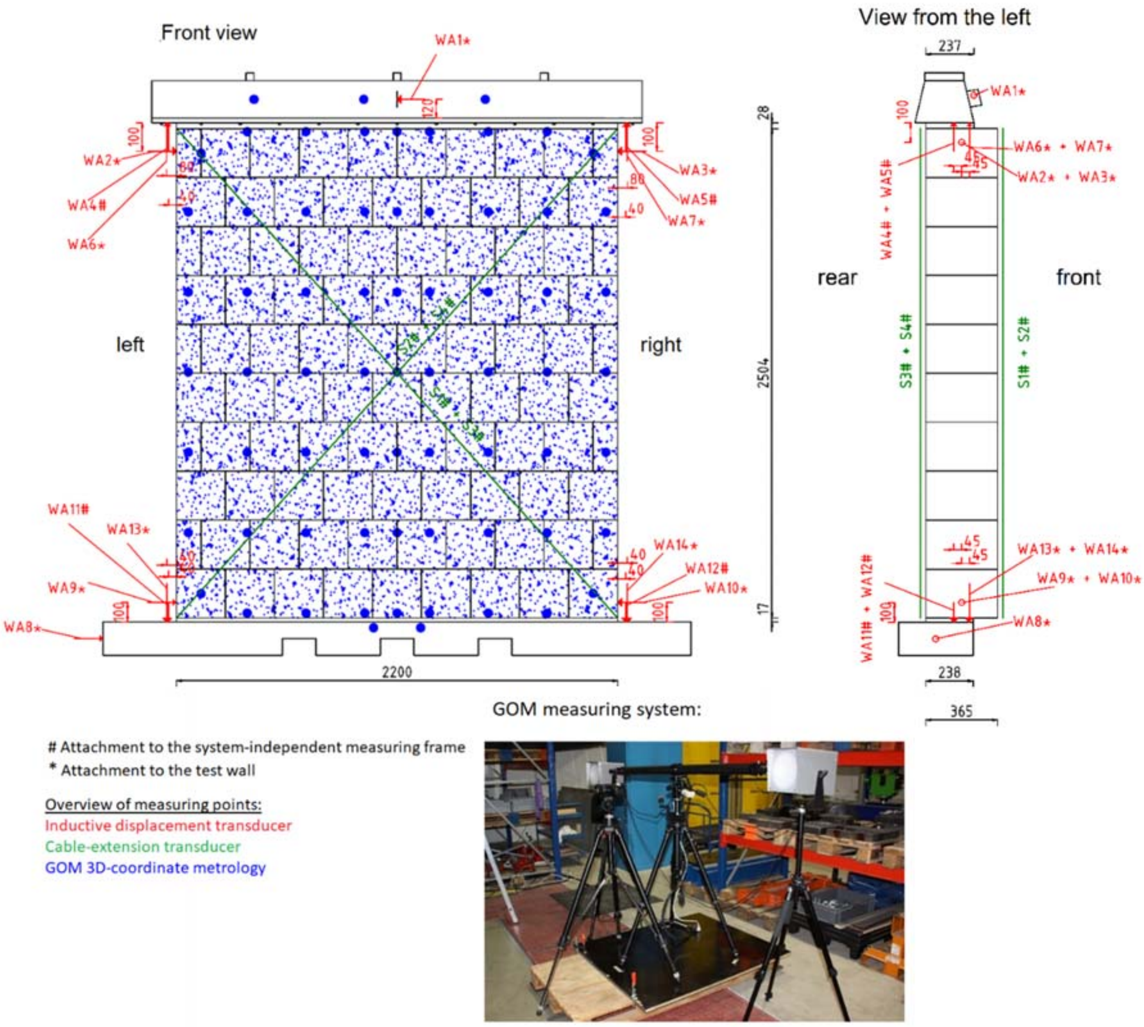

Fig. 5 Measuring points and typical wall geometry with optical measuring system

TABLE I
SUMMARY OF TEST RESULTS

Wall specimen properties					Relevant horizontal forces			EC 6/NA (D) [5]	Bilinearized load deflection curve			
	Type of bed joint	Wall length l [m]	Slab bearing length t_A [%]	Vertical load p [kN/m]	Maximum horizontal force $F_{h,max}$ [kN] (mean value)	Corresponding position of the zero crossing of the bending moment ψ [-] (mean value)	Corresponding storey displacement d [mm] (mean value)	Norm. Resist. V_{Rk} [kN]	Plastic horizontal force $F_{h,u}$ [kN]	Elastic storey displacement d_e [mm]	Plastic storey displacement d_u [mm]	Ductility μ [-]
W1.t	TBM	2,20	100	155	168,5	0,44	11,74	122,00	160,9	1,73	13,68	7,9
W1.3					159,6	0,66	13,76	115,00	154,9	5,80	15,41	2,7
W2.1	TBM	2,20	100	60	75,4	0,46	3,45	71,60	70,5	1,32	20,23	15,4
W2.2				130	139,3	0,44	10,92	111,00	132,2	3,39	13,27	3,9
W3	TBM	2,20	66	130	133,9	0,43	9,05	110,00	127,1	2,38	10,08	4,2
W4	PU	2,20	66	130	123,4	0,44	4,91	111,00	113,2	2,33	6,57	2,8
W5	PU	2,19	100	60	81,9	0,47	2,85	72,30	72,5	1,51	11,45	7,6
W6	PU	2,20	100	130	125,4	0,45	6,50	112,00	115,7	2,34	7,98	3,4
W7	PU	2,20	66	30	51,1	0,47	2,73	46,60	39,7	1,10	10,35	9,4

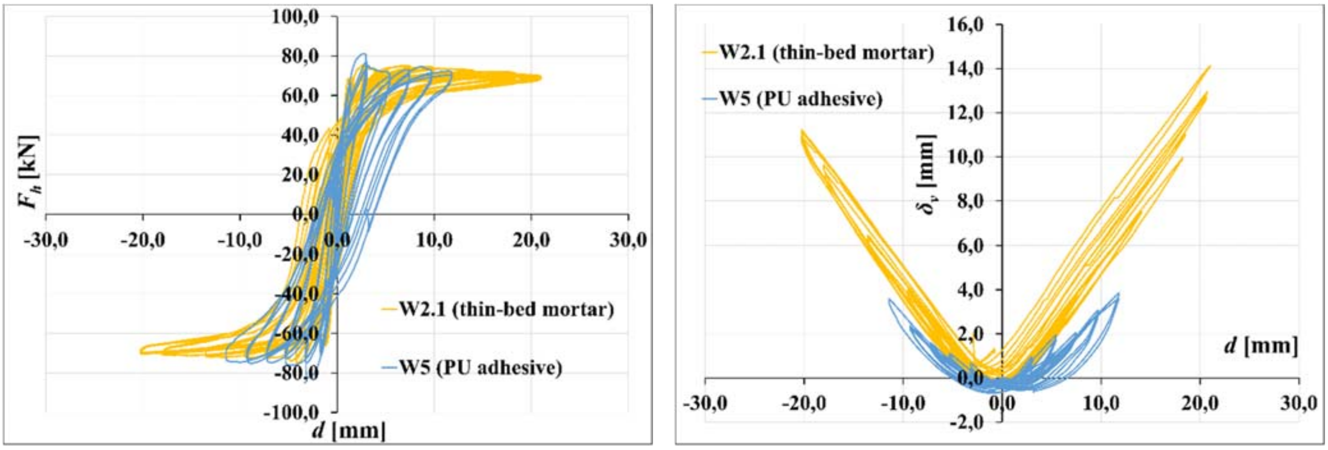

(a) Hysteresis (b) Vertical and horizontal displacement of the head of the walls

Fig. 6 Test walls W2.1 and W5

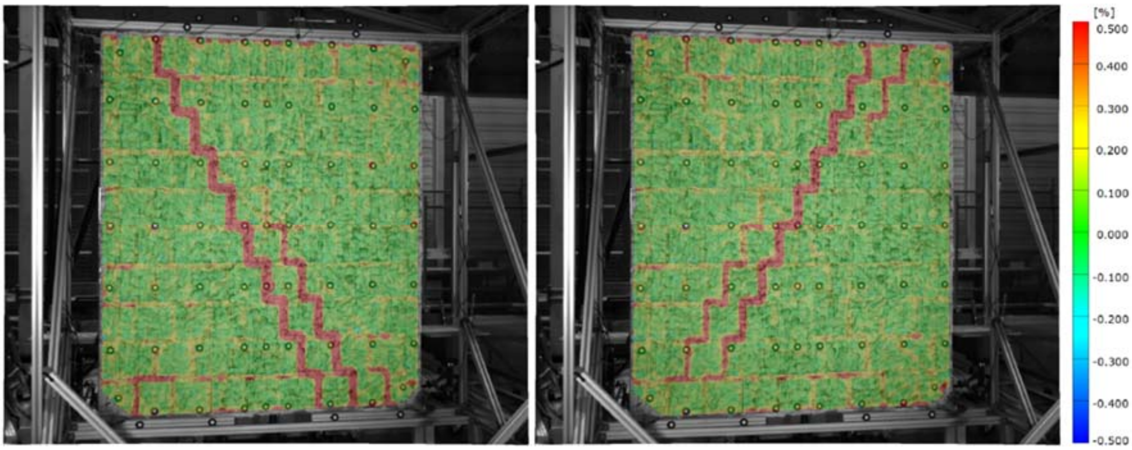

(a) W2.1: Main strain distribution at minimum negative horizontal force and main strain distribution at maximum positive horizontal force

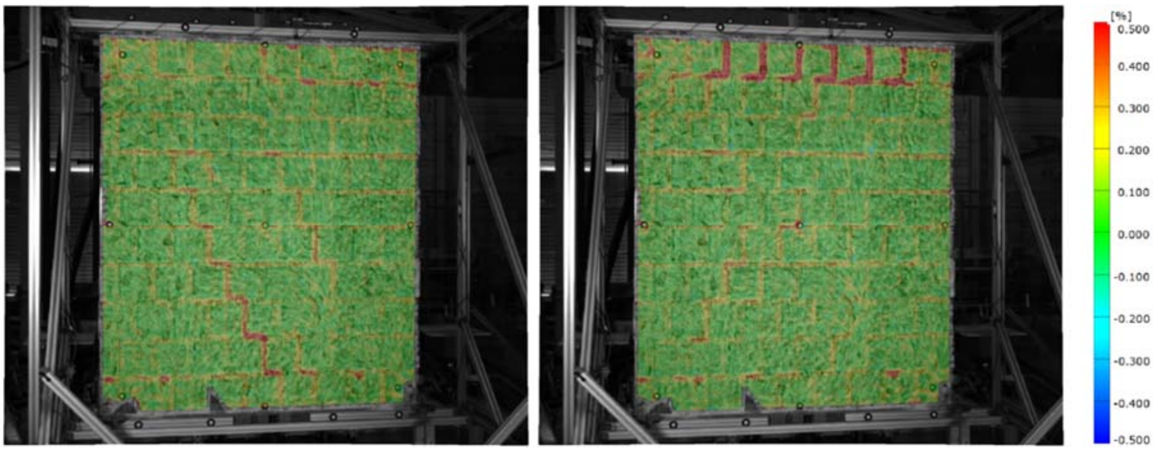

(b) W5: Main strain distribution at minimum negative horizontal force and main strain distribution at maximum positive horizontal force

Fig. 7 Main strain distributions of test walls W2.1 and W5

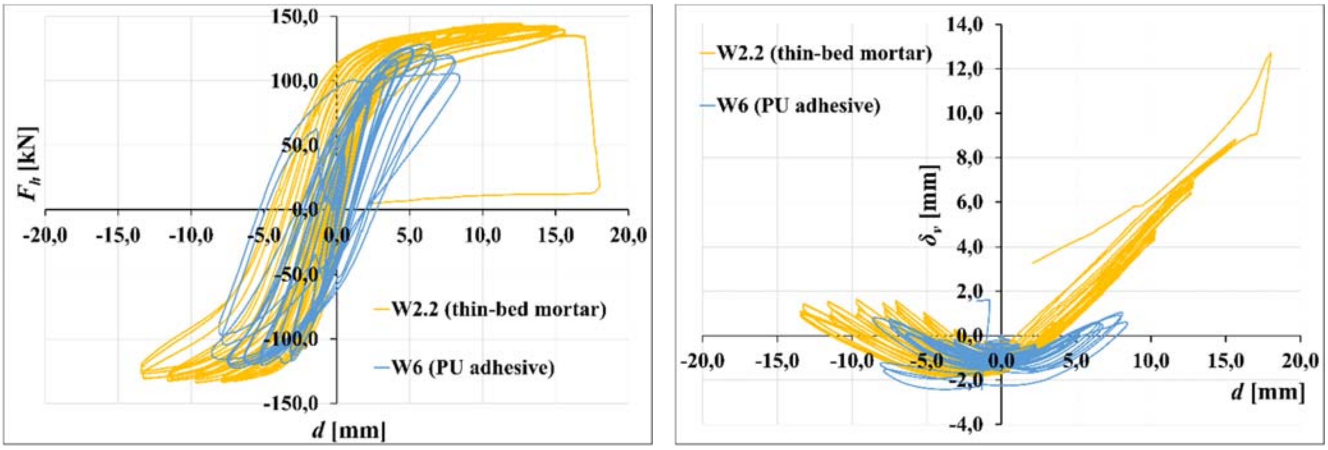

(a) Hysteresis (b) Vertical and horizontal displacement of the head of the walls

Fig. 8 Test walls W2.2 and W6 (W2.2 is a follow up test on the same specimen as test W2.1; therefore, previous damage can be assumed)

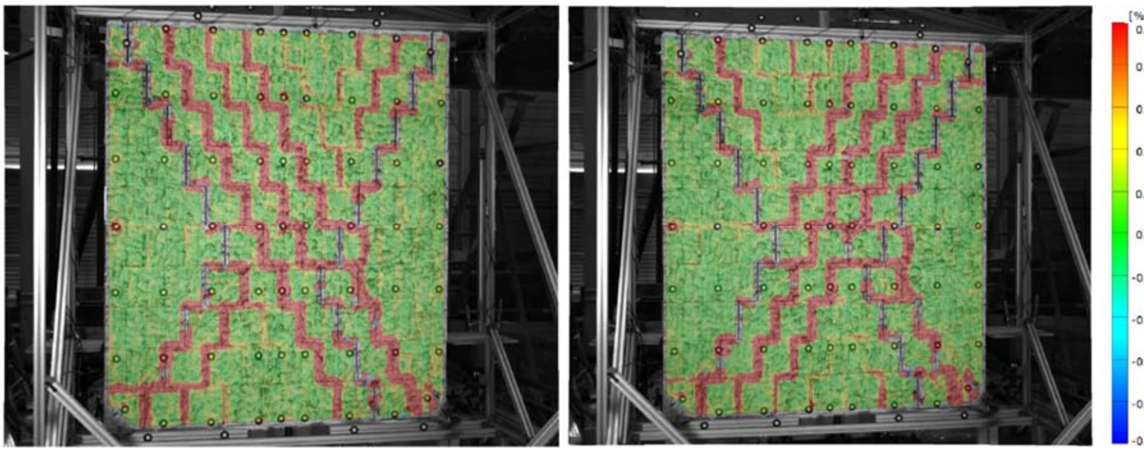

a) W2.2: Main strain distribution at minimum negative horizontal force and main strain distribution at maximum positive horizontal force

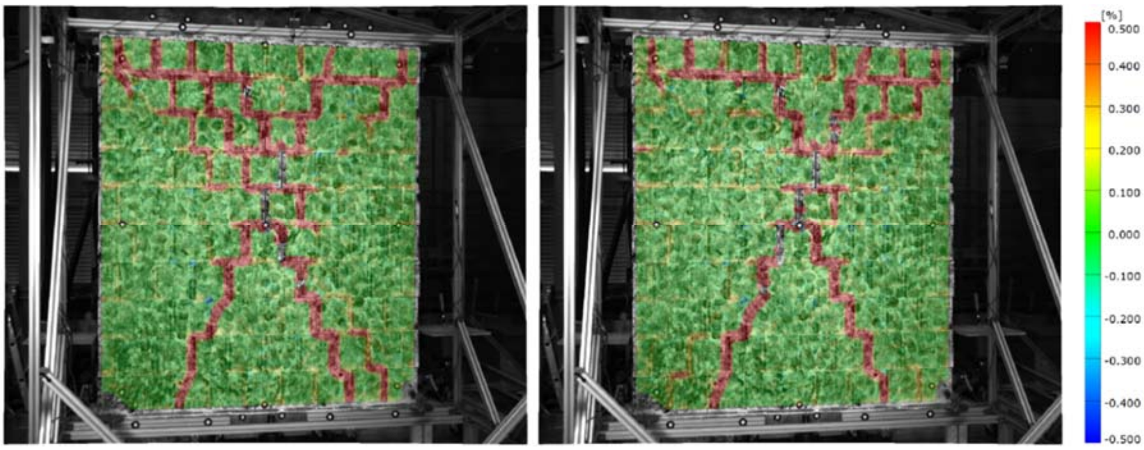

b) W6: Main strain distribution at minimum negative horizontal force and main strain distribution at maximum positive horizontal force

Fig. 9 Main strain distributions of test walls W2.2 and W6

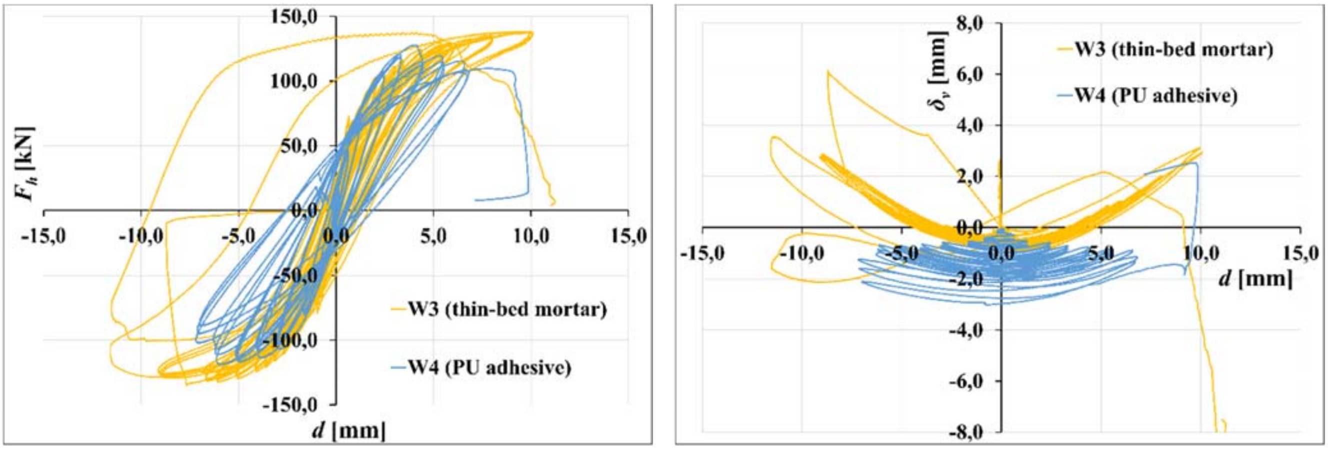

(a) Hysteresis (b) Vertical and horizontal displacement of the head of the walls

Fig. 10 Test walls W3 and W4

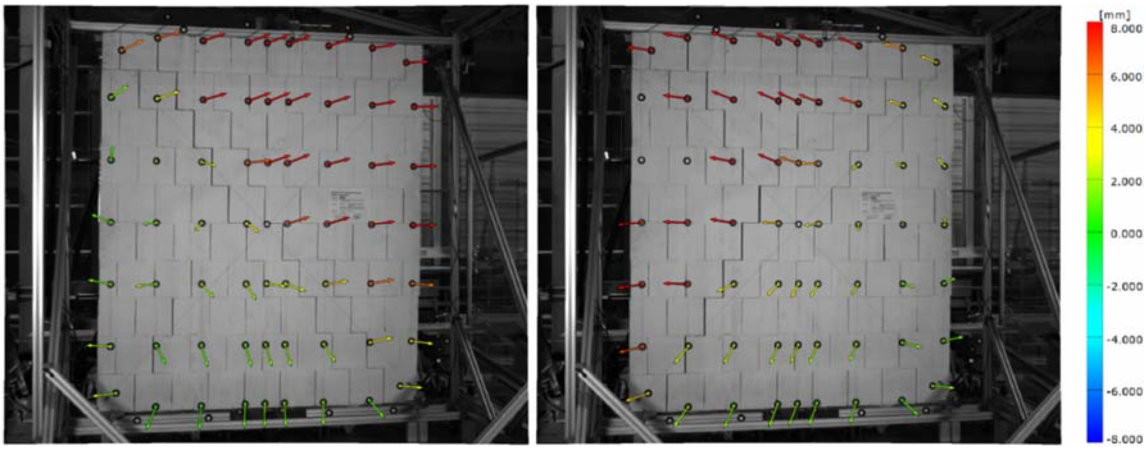

(a) W3: Displacements of wall surface at minimum negative horizontal force and Displacements of wall surface at maximum positive horizontal force

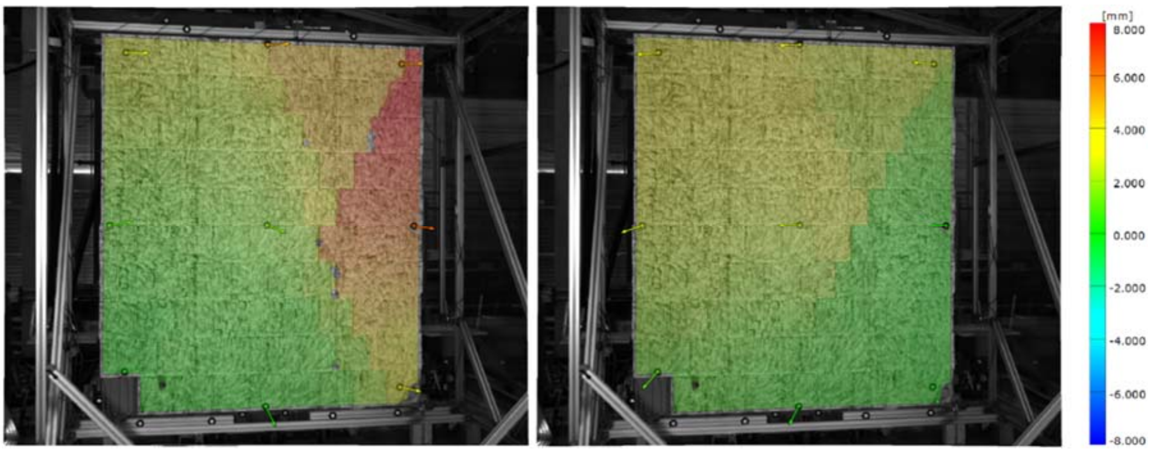

(b) W4: Displacements of wall surfaces at minimum negative horizontal force and Displacements of wall surfaces at maximum positive horizontal force

Fig. 11 Displacements of wall surfaces of test walls W3 and W4

V. Interpretation of the Results Regarding the Influence of the Bed Joint Type

While the deformability of the TBM walls exceeds that of the glued masonry walls by at least 50% in the three test pairs measured in the linearized equivalent curves, the maximum load-bearing capacities are close together. With low vertical loading (60 kN/m), the maximum load-bearing capacity of the glued masonry walls is slightly higher than that of the thin-bed walls. With increasing load (130 kN/m) the opposite is true, whereby the difference between both masonry types is higher, as shown in Fig. 12.

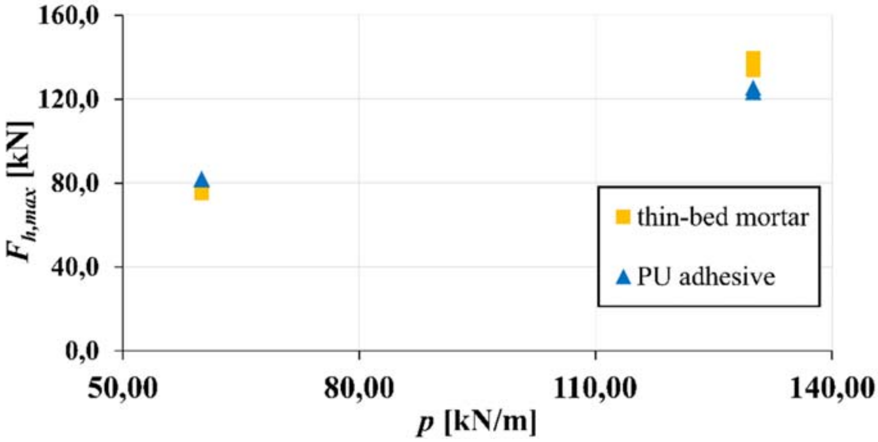

Fig. 12 Maximum horizontal force $F_{h,max}$ (mean value) versus vertical load p (W2.1 to W6)

These differences in deformation capacity and load-bearing capacity can be attributed to differences in the adhesive strength f_v and friction value α of the two connectors. Of course, the small differences in the horizontal load-bearing capacity, can also be due to natural fluctuations, which cannot be ruled out due to the small number of tests. Brahmeshuber and Graubohm report in [8] adhesive shear tests according to DIN EN 1052-3 [9] carried out on test specimens made of vertical perforated bricks, which were also manufactured using the same PU adhesive construction method examined here. In addition, reference tests were also run on masonry using the TBM. The following Coulomb static friction relationships were derived by Brahmeshuber and Graubohm from mean values: [8]

$$f_{v,PU} = f_{v,0,PU} + \alpha_{PU} \cdot \sigma_N = 0.22 + 0.451 \cdot \sigma_N \quad (1)$$

$$f_{v,TBM} = f_{v,0,TBM} + \alpha_{TBM} \cdot \sigma_N = 0.37 + 0.792 \cdot \sigma_N \quad (2)$$

The coefficient of friction α of the thin-bed masonry was about 75% higher than that of the glued masonry. When determining the initial shear strength $f_{v,0}$ it should be noted that this parameter is often subject to greater scatter than the coefficient of friction and is also dependent on the type of stone and its hole pattern. The selected test method (with or without ballasting) and the application of prestressing immediately after the test specimen has been manufactured also have a decisive influence on both the TBM and the adhesive.

In a total of eight side tests at the University of Kassel on the batch of bricks examined here, the average initial shear strength for thin-bed masonry was $f_{v,0,TBM}$= 0.26 N/mm^2 and for glued masonry $f_{v,0,PU}$= 0.39 N/mm^2. The difference to [8] for the thin-bed masonry can possibly be explained by the different tested stone-types and especially by different storage conditions. To ensure comparable conditions to the test walls, the small specimens were stored together with the test walls at an average humidity of 44%. In [8] the test specimens were stored under controlled laboratory conditions at 20° and a humidity of 65%. The deviations for the glued masonry can be explained by differences in the hole pattern and thus in the quantity and distribution of the glue applied.

An attempt to back-calculate the initial shear strength and the coefficient of friction based on the wall tests assuming frictional failure resulted in significantly differing values, which were associated with a high degree of scatter, which is why they are not explained in more detail here.

Assuming a primary shear failure through friction, especially in the first two full supported pairs of tests, and a Coulomb static friction relationship with lower initial shear strength but higher coefficient of friction for the TBM than for the glued masonry, the differences in the load-bearing capacities can be explained with the following assumptions: At higher loads (130 kN/m), the static friction resistance, which is dependent on the normal force, has a higher proportion of the total shear resistance. This explains the higher shear capacity at higher loads. The reverse is the case with low loads. The influence of the initial shear strength on the total shear resistance increases and explains the slightly higher shear resistance of the glued masonry, as shown in Fig. 12.

The consistently lower deformation capacity of the glued masonry can also be explained by differences in the initial shear strength and friction parameter of the glued masonry, which deviate from those of the thin-bed masonry, whereby the different adhesive tensile strength must also be taken into account as a key influencing variable here.

In contrast to the load-bearing capacity, the deformation capacity of masonry panels cannot be predicted directly from the failure mode that governs the maximum load-bearing capacity. The total deformation at the top of the wall is essentially made up of a bending component (rocking) and a shear component. Because even in the event of a shear failure, the wall can be deformed in bending by tearing open the most distant bed joints until the load-bearing capacity at shear failure is reached.

If the bending portion of the total deformation predominates, this usually has a favorable effect on the deformation capacity, since the wall usually remains intact up to the bending compression failure and largely behaves more like a rotating rigid body. In contrast, a dominant shear/friction deformation often leads to a lower deformation capacity, since the load transfer changes locally due to the opening head joints and stone cracks, and the deformation capacity is thus already achieved at lower values.

The secondary bending failure is the reason for the greater deformability of the thin-bed masonry observed in the tests. After the thin-bed masonry has reached its maximum shear resistance due to shear friction failure and the initial shear strength then decreases, the load-bearing capacity drops only slightly. Due to shear failure, the wall is divided diagonally into two wedges, of which one of the two wedges now performs an independent rotational movement depending on the direction of the force, as can be seen from the higher vertical displacement of the wall head of the TBM walls in Figs. 6, 8, 10. Individual stone steps are formed within the rotating wedge, some of which rotate independently of one another around the foot of the wall and move upwards with different vertical distances. One reason for this behavior is the low adhesive tensile strength of the mortar. This leads to primary shear failure followed by secondary flexural failure. During the rotation, the vertical loading is probably transferred to the rotating wedge. The ultimate load due to flexural failure of the wedge is therefore lower than the remaining frictional resistance in the bed joints of the rotating wedge. In tests W2.2 and W3, the load-bearing capacity also increases with increasing deformation. Due to the secondary bending failure, the hysteresis remains constricted in the TBM masonry wall tests.

In case of the glued masonry tests, a secondary bending behavior is only very slight. On the one hand, the normal force-dependent static friction resistance of the glued masonry examined is lower than that of the TBM masonry, as described above. On the other hand, the adhesion tensile strength of the PU adhesive is probably significantly higher than that of TBM, as tests on the flexural strength by [8]. There, the flexural strength of the glued masonry perpendicular to the horizontal joint was around a factor of 1.5 higher than that of the thin-bed masonry. The demolition work on the test walls following the tests in Kassel also confirms the higher flexural strength. The glued test walls were much more difficult to tear off, since many of the bricks were still firmly connected.

The bending resistance of the separated wall wedge after primary shear friction failure is therefore greater in the glued masonry than the remaining static friction resistance. The wall therefore performs a sliding movement. The head joints and thus also the hysteresis open further. Although the energy dissipation is greater, the ductility of the wall is lower.

VI. Conclusion

While the load-bearing capacities between glued and mortared masonry hardly differed in the tests carried out, the deformability of the TBM masonry turned out to be significantly higher. It could be shown that the differences can be traced back to the coefficients of adhesion and friction of both composite materials. The adhesive strengths, i.e. adhesive shear and adhesive tensile strengths, of the PU adhesive are probably higher than those of the TBM. In contrast, the TBM masonry had a higher frictional resistance. As a consequence of the different material parameters of the mortar, the tested TBM walls were able to develop a secondary flexural failure after a primary shear failure, which could not occur to this extent in the glued masonry due to the lower friction resistance and the significantly higher adhesive strength. The deformation capacity of the glued masonry is therefore less but also significantly fuller. The extent to which the associated greater hysteresis damping of the glued masonry can compensate for the lower ductility with regard to earthquake safety remains open.

References

[1] E. Fehling, P. Capewell, "Schubversuche an Mauerwerksscheiben (Redbloc Systemwände)" (unpublished test report). Kassel: University of Kassel, 2023.

[2] DIN EN 772-1:2016-05. Prüfverfahren für Mauersteine – Teil 1: Bestimmung der Druckfestigkeit. Berlin: Normenausschuss für Bauwesen (NABau) im DIN Deutsches Institut für Normung e. V. Hrsg., Beuth Verlag GmbH, 2017.

[3] DIN EN 1052-1:1998-12. Prüfverfahren für Mauerwerk – Teil 1: Bestimmung der Druckfestigkeit. Berlin: Normenausschuss für Bauwesen (NABau) im DIN Deutsches Institut für Normung e. V. Hrsg., Beuth Verlag GmbH, 1998

[4] https://www.redbloc.at/produktion-montage/produktionsschritte/ (Retrieval Date: 10.02.2024)

[5] C. Alfes, W. Brameshuber, C.-A. Graubner, W. Jäger, W. Seim, "Der Eurocode 6 für Deutschland - DIN EN 1996: Bemessung und Konstruktion von Mauerwerksbauten mit Nationalen Anhängen – Kommentierte Fassung“, Ernst & Sohn Verlag für Architektur und technische Wissenschaften GmbH & Co. KG, 2013.

[6] M. Tomazevic, M., "Earthquake-Resistant Design of Masonry Buildings”, London: Imperial College Press, 1999,

[7] T. Pfetzing, "Zur Schubtragfähigkeit von Mauerwerksscheiben mit teilweise aufliegender Deckenplatte" (thesis). Kassel: Kassel University press, 2021.

[8] W. Brameshuber, M. Graubohm, "Prefabricated masonry panel system with two-component polyurethane adhesive", Berlin: Mauerwerk 19 (2015), Heft 1, Ernst & Sohn Verlag für Architektur und technische Wissenschaften GmbH & Co. KG, 2015.

[9] DIN EN 1052-3:2007-06. Prüfverfahren für Mauerwerk – Teil 3: Bestimmung der Anfangsscherfestigkeit (Haftscherfestigkeit). Berlin: Normenausschuss für Bauwesen (NABau) im DIN Deutsches Institut für Normung e. V. Hrsg., Beuth Verlag GmbH, 1998